

Magnetization reversal in magnetostatically coupled dot arrays

著者	北上 修
journal or publication title	Journal of Applied Physics
volume	91
number	10
page range	6952-6954
year	2002
URL	http://hdl.handle.net/10097/47664

doi: 10.1063/1.1450840

Magnetization reversal in magnetostatically coupled dot arrays

H. Shima

Department of Materials Science, Graduate School of Engineering, Tohoku University, Sendai 980-8579, Japan and JST, Japan Science and Technology Corporation, CREST, Kawaguchi 3320012, Japan

K. Yu. Guslienko^{a)}

School of Physics, Korea Institute for Advanced Study, Seoul 130-012, Korea

V. Novosad^{b)}

Department of Materials Science, Graduate School of Engineering, Tohoku University, Sendai 980-8579, Japan and Materials Science Division, Argonne National Laboratory, Argonne, Illinois 60439

Y. Otani

Department of Materials Science, Graduate School of Engineering, Tohoku University, Sendai 980-8579, Japan and JST, Japan Science and Technology Corporation, CREST, Kawaguchi 3320012, Japan

K. Fukamichi

Department of Materials Science, Graduate School of Engineering, Tohoku University, Sendai 980-8579, Japan

N. Kikuchi, O. Kitakami, and Y. Shimada

IMRAM, Tohoku University, Sendai 980-8577, Japan

The submicron permalloy dots with variable diameter and interdot distance were microfabricated into a rectangular lattice by means of *e*-beam lithography and lift-off techniques. The hysteresis loops exhibit characteristic magnetization reversal accompanied by “nucleation” and “annihilation” of magnetic vortices inside the dots. The magnetic response of the samples with well-separated elements is isotropic in the plane. The arrays with a small interdot distance show magnetic anisotropy with the easy axis along the shortest period in the array. This anisotropy is originated from the interdot magnetostatic interaction. In the closely packed (when interdot distance is smaller than dot radius) arrays so that $d/R < 1$, the magnetostatic interaction decreases the vortex nucleation and annihilation fields, and increases the initial susceptibility. © 2002 American Institute of Physics. [DOI: 10.1063/1.1450840]

The arrays of submicron size ferromagnetic particles draw much attention because of their possible potential as magnetic storage media¹ as well as a model system for studying magnetization reversal processes.² Small dots reveal a single-domain state to reduce exchange energy, but nonuniform magnetic states stabilize as the dot sizes are increased. For example, an isolated polycrystalline ferromagnetic disk-shaped dot with submicron diameters and thickness of several 10 nanometers exhibits a vortex-type spin structure with a closure flux in remanence.^{3–7} The magnetic behavior of dot arrays is defined by the dot individual properties for well-separated magnetic elements, whereas the interdot magnetostatic interaction becomes essential for the dot arrays with small interdot distances.^{8–11} In the present work we report the experimental results of magnetization reversal in submicron circular permalloy (Py, Fe₈₁Ni₁₉) dots arranged into rectangular lattices, wherein the magnetization reversal accompanies nucleation, displacement, and annihilation of magnetic vortices. We will show that the magnetostatic in-

teraction plays an important role in determining the magnetization reversal for the arrays with a small interdot distance, leading to considerable decreases in the vortex nucleation H_n and annihilation H_{an} fields, and an increase in initial in-plane susceptibility $\chi(0)$.

The arrays of circular Py dots were prepared using microfabrication techniques as follows. First a standard silicon wafer is spin coated with a positive photoresist. Next, the desired patterns are then defined by *e*-beam lithography. The magnetic film is deposited in vacuum on the water-cooled substrate from a Py target. Finally, after ultrasonic assisted lift-off process, we obtained the arrays of circular dots arranged into rectangular lattices with variable diameter and interdot distance. The orientation of the lattice is shown in Fig. 1. The dot thickness L is about 80 nm and diameters $2R$ are chosen to be 0.4 μm , 0.6 μm , and 0.8 μm . For studying the effect of magnetostatic interdot interaction, the distance between edges of neighboring elements d was varied from 30 nm to 1 μm . We prepared two kinds of rectangular dot arrays: (A) interdot distance d_x parallel to Ox axis is variable and decreases from $2R$ to almost zero, whereas $d_y = 2R$ is constant; (B) $d_x = R/2$ is constant, d_y decreases from $3R$ to $R/2$ (square array), $R = 0.4 \mu\text{m}$. The microfabricated circular

^{a)}Present address: Seagate Research, Pittsburgh, PA 15203.

^{b)}Author to whom correspondence should be addressed; electronic mail: novosad@anl.gov

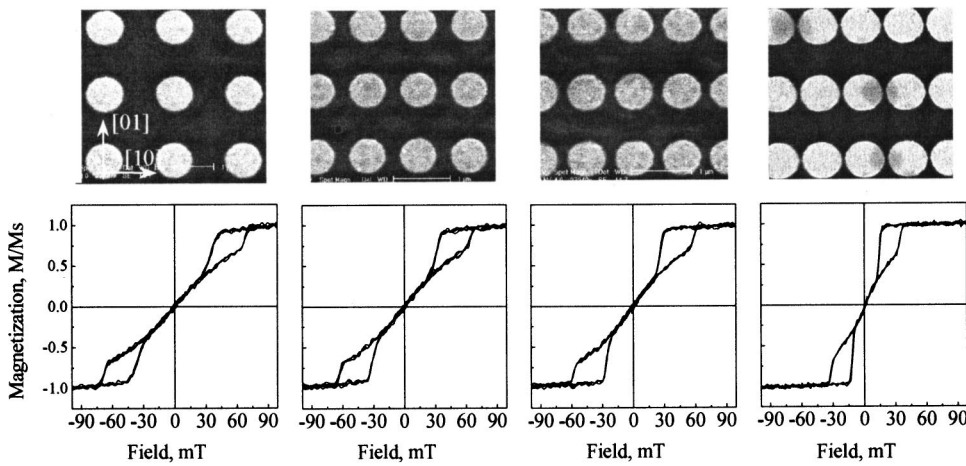


FIG. 1. The scanning electron microscope images and corresponding hysteresis loops of the microfabricated permalloy dot arrays with dot diameter $2R=0.8\ \mu\text{m}$, thickness $L=80\ \text{nm}$, and variable interdot distance d .

dots have sharp edges and are almost identical, as confirmed by an *ex situ* atomic force microscope (AFM), a scanning electron microscope (SEM), and a magnetic force microscope (MFM). The hysteresis loops were traced using a magneto-optical technique and a resonating sample magnetometer (RSM) for different orientations of the dot arrays with respect to the in-plane applied magnetic field.

Figure 1 shows SEM images and corresponding hysteresis loops measured along the [01] lattice direction of the A-type dot arrays with diameter of $0.6\ \mu\text{m}$ and variable interdot distances. The magnetization reversal process is observed to accompany the “nucleation” and “annihilation” of magnetic vortices.^{6,7} With decreasing field from the saturated state, the magnetization gradually decreases, showing an abrupt jump at the nucleation field H_n . In this field a single magnetic vortex is formed in each dot. In the remanent state, the vortex stays at the center of the dot, as confirmed by MFM imaging. When the external magnetic field is applied, the vortex core is displaced to increase the average magnetization component along the field direction according to the balance between the magnetostatic and Zeeman energies. At the annihilation field H_{an} , the vortex vanishes and turns to a single-domain state. The dot-to-dot geometry and the crystal structure variations broaden the distribution of the vortex nucleation and annihilation fields. The microfabrication processes for all samples are identical. Therefore, the intrinsic distribution of H_n and H_{an} has to be of the same order for both magnetostatically isolated and coupled dot arrays. This fact was confirmed by directly comparing the broadening of switching fields normalized by their average values for the samples with different diameters and interdot distances. This contrasts with the experimental data reported for rectangular Py particles, where the distribution in switching field was found to get narrower due to the magnetostatic interaction between the elements.¹¹ Note that structural or microstructural defects have stronger influence to broadening of nucleation field than the annihilation field values. As seen from Fig. 1, the switching fields and the slope of the linear part of hysteresis loops depend on the interdot distance.

Figure 2 summarizes the experimental data for the magnetostatically induced anisotropy constant K_u and the vortex annihilation field in the A-type arrays with the variable interdot distance d_x . The value of d_y was kept constant and equal

to the dot diameters. The magnetic field is applied along the (Ref. 10) axis. The values of H_{an} and H_n are normalized to their values measured in arrays of well-separated dots ($d_x, d_y \gg R$), and the interdot distance is shown in reduced units $\delta = d/R$. The anisotropy constant was determined as $K_u = \Delta H_{an} M_s / 2$, where $\Delta H_{an} = H_{an}(\text{isol}) - H_{an}$ is the difference between the annihilation fields in arrays of isolated and coupled dots. $M_s = 8.6 \times 10^5\ \text{J/m}$ is the magnetization of saturation for permalloy. The magnetostatic interdot interaction is important in the magnetization reversal for arrays with $\delta = d/R < 0.5$, leading to a decrease in both, nucleation and annihilation fields. Similar results were obtained with micro-magnetic calculations for the chain of ferromagnetic disks.¹²

The closure of the magnetic flux structure, that is realized in circular ferromagnetic dots with vortex spin distribution, suggests that dots are not interacting in remanence. The contribution of the out-of-plane magnetization component in the vortex core can be ignored, because the vortex core radius, being approximately equal to exchange length, is small in comparison to the in-plane dot size. However, field-driven displacement of the vortices results in a non-negligible stray field around the dot, which defines the strength of interdot

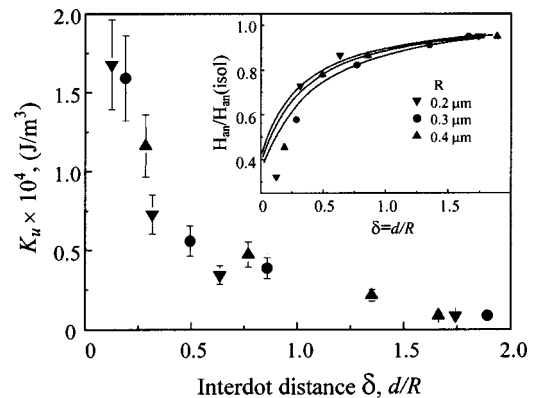


FIG. 2. The magnetostatically induced anisotropy constant K_u vs the normalized interdot distance $\delta = d/R$. The inset shows scaled annihilation fields $H_{an}/H_{an}(\text{isol})$ determined by the experiment (markers) and the calculation (lines) vs the normalized interdot distance $\delta = d/R$. Solid lines are calculated using Eq. (1). The different solid lines correspond to $\beta=0.40$ (lower curve), 0.27, 0.20 (upper curve). Field is applied along the [10] dot lattice direction.

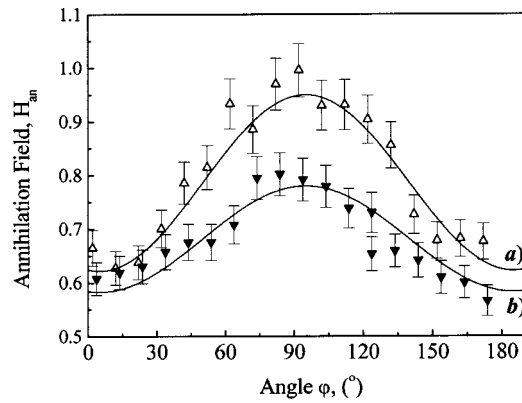


FIG. 3. Angular variation of the annihilation field H_{an} measured for two different dot arrays of B type with dot diameter $0.8 \mu\text{m}$ and interdot distances: (a) $d_x=0.2 \mu\text{m}$, $d_y=1.2 \mu\text{m}$ and (b) $d_x=0.2 \mu\text{m}$, $d_y=0.4 \mu\text{m}$.

magnetostatic coupling. The magnetic properties of identical interacting dots can be modeled analytically on the basis of a “rigid vortex” model.⁶ This model assumes that the vortex moves in the in-plane applied magnetic fields while keeping its shape. The reduced equilibrium core displacement $s = l/R$ is determined by minimizing the total magnetic energy as a function of the dot sizes and interdot distances. In external magnetic field, the dot energy consists of exchange W_{ex} , Zeeman W_H , and magnetostatic W_m contributions. The exchange and Zeeman terms are not affected by interdot magnetostatic coupling, and hence are the same as those for an array of isolated dots. The energy of magnetostatic coupling in two-dimensional arrays of identical circular dot arrays can be calculated starting from the general expression for the magnetostatic energy density of an in-plane magnetized patterned film.^{9,10} The following expression for the annihilation field can be deduced:

$$H_{an}(\beta, \delta, R, \varphi_H) = 2\Gamma(\beta, \delta, R, \varphi_H)M_s, \quad (1)$$

$$\Gamma(\beta, \delta, R, \varphi_H) = \frac{4\pi}{T_x T_y} \sum_{\mathbf{k}} f(\beta k R) \frac{J_1^2(kR)}{k^2} \cos^2(\varphi_{\mathbf{k}} - \varphi_H) - \frac{1}{2} \left(\frac{R_0}{R} \right)^2,$$

where $f(x) = 1 - (1 - \exp(-x))/x$, $\beta = L/R$ is the dot aspect ratio, $J_1(x)$ is the Bessel function, and $\varphi_{\mathbf{k}}$ and φ_H are, respectively, the polar angles for the reciprocal lattice vector \mathbf{k} and applied field \mathbf{H} , $T_{x,y} = 2R + d_{x,y}$ are the dot lattice periods, R_0 is the exchange length. The function $\Gamma(\beta, \delta, R, \varphi_H)$ defines angular variation of magnetostatically induced anisotropy. The in-plane initial susceptibility is $\chi(0) = (2\Gamma)^{-1}$ within the “rigid vortex” model, i.e., it is inversely proportional to H_{an} . The annihilation fields calculated using Eq. (1) (lines) are compared directly to the experimental data (symbols) in the inset of Fig. 2. The same effect of reducing of the vortex nucleation field with decreasing interdot distance was observed and will be reported elsewhere.

The magnetization curve of the rectangular array (B -type) depends on the angle between the external field and the lattice orientation. Figure 3 shows the angular variation of

annihilation field H_{an} measured for two kinds of rectangular dot arrays with the dot diameter of $0.8 \mu\text{m}$ and the same interdot distance along the $[10]$ lattice direction, but with different distances along the $[01]$ direction, ($d_x=0.2 \mu\text{m}$, $d_y=1.2 \mu\text{m}$, and $d_y=0.4 \mu\text{m}$). Therefore, these two samples can be viewed as a chain and an array of the dots. The variation of annihilation field can be well approximated to the $\sin^2(\varphi)$ function (solid lines), suggesting that both samples have a uniaxial magnetic anisotropy. The easy magnetization axis is parallel to the row of dots with smallest interdot spacing. We found that the rule predicted by the “rigid vortex” model $\chi(0)H_{an} \approx \text{const}$ fulfills at changing of the in-plane field angle φ_H . The chain, wherein the interdot magnetostatic interaction is more important along one axis than the other, shows stronger coupling effects on the magnetization reversal. The hysteresis loops measured along the hard axis are almost identical to those for the arrays of isolated dots with the same geometry. In the case of rectangular dot arrays, the interdot magnetostatic contributions along different directions are competing, and, as a result, the magnetic anisotropy due to magnetostatic coupling becomes weaker. Finally, square arrays of circular dots with $d_x=d_y=0 \mu\text{m}$ show no in-plane anisotropy, similar to the arrays of magnetostatically isolated dots. We have not found so far any four-fold magnetic anisotropy for the square array as it was reported in Ref. 13 for the FeNi dot arrays with similar parameters. Equation (1) was obtained in the dipolar approximation. For the considered rectangular arrays near saturation ($H=H_{an}$), the in-dot quadrupole moments are not so important because of the dominant interdot dipolar coupling.

This work was supported in part by Korea Institute for Advanced Study, RFTF of JSPS and the Grant-in-Aid for Scientific Research from the Ministry of Education, Science, and Culture in Japan. Work at ANL was supported by U.S. Department of Energy, BES Materials Sciences under Contract No. W-31-109-ENG-38.

- ¹C. A. Ross, *Annu. Rev. Mater. Sci.* **31**, 203 (2001).
- ²A. Aharoni, *Introduction to the Theory of Ferromagnetism* (Oxford University Press, New York, 2001), p. 336.
- ³R. P. Cowburn, D. K. Koltsov, and A. O. Adeyeye, *Phys. Rev. Lett.* **83**, 1042 (1999).
- ⁴J. Raabe, R. Pulwey, R. Sattler, T. Schweinbock, J. Zweck, and D. Weiss, *J. Appl. Phys.* **88**, 4437 (2000).
- ⁵T. Shinjo, T. Okuno, R. Hassdorf, K. Shiget, and T. Ohno, *Science* **289**, 5481 (2000).
- ⁶K. Yu. Guslienko, V. Novosad, Y. Otani, H. Shima, and K. Fukamichi, *Appl. Phys. Lett.* **78**, 3848 (2001).
- ⁷V. Novosad, K. Yu. Guslienko, Y. Otani, H. Shima, K. Fukamichi, N. Kikuchi, O. Kitakami, and Y. Shimada, *IEEE Trans. Magn.* **EMG-37**, 2088 (2001).
- ⁸R. P. Cowburn, A. O. Adeyeye, and M. E. Welland, *New J. Phys.* **1**, 16 (1999).
- ⁹K. Yu. Guslienko, *Appl. Phys. Lett.* **75**, 394 (1999).
- ¹⁰E. Y. Tsymbal, *Appl. Phys. Lett.* **77**, 2740 (2000).
- ¹¹K. J. Kirk, J. N. Chapman, S. McVitie, and R. P. Aitchison, *J. Appl. Phys.* **87**, 5105 (2000).
- ¹²K. Yu. Guslienko, V. Novosad, Y. Otani, H. Shima, and K. Fukamichi, *Phys. Rev. B* **65**, 24414 (2002).
- ¹³C. Mathieu, C. Hartmann, M. Bauer, O. Buettner, S. Riedling, B. Roos, S. O. Demokritov, B. Hillebrands, B. Bartenlian, C. Chappert, D. Decanini, F. Rousseaux, Cambil, A. Müller, B. Hoffmann, and U. Hartmann, *Appl. Phys. Lett.* **70**, 2912 (1997).